Biosensors and Bioelectronics 64 (2015) 386–391

Contents lists available at ScienceDirect

Biosensors and Bioelectronics

journal homepage: www.elsevier.com/locate/bios

Short communication

A label-free ultrasensitive electrochemical DNA sensor based on thin-layer MoS_2 nanosheets with high electrochemical activity

Xinxing Wang [a], Fuxin Nan [a], Jinlong Zhao [a], Tao Yang [a,*], Tong Ge [b], Kui Jiao [a,*]

[a] Key Laboratory of Sensor Analysis of Tumor Marker of Education Ministry, College of Chemistry and Molecular Engineering, Qingdao University of Science and Technology, Qingdao 266042, PR China

[b] Huangdao Entry-Exit Inspection and Quarantine Bureau, Qingdao 266555, PR China

ARTICLE INFO

Article history:
Received 13 July 2014
Received in revised form
2 September 2014
Accepted 4 September 2014
Available online 18 September 2014

Keywords:
Thin-layer MoS_2 nanosheets
High electrochemical activity
Electrochemical DNA sensor
Label-free
Ultrasensitive

ABSTRACT

A label-free and ultrasensitive electrochemical DNA biosensor, based on thin-layer molybdenum disulfide (MoS_2) nanosheets sensing platform and differential pulse voltammetry detection, is constructed in this paper. The thin-layer MoS_2 nanosheets were prepared via a simple ultrasound exfoliation method from bulk MoS_2, which is simpler and no distortion compared with mechanical cleavage and lithium intercalation. Most importantly, this procedure allows the formation of MoS_2 with enhanced electrochemical activity. Based on the high electrochemical activity and different affinity toward ssDNA versus dsDNA of the thin-layer MoS_2 nanosheets sensing platform, the *tlh* gene sequence assay can be performed label-freely from 1.0×10^{-16} M to 1.0×10^{-10} M with a detection limit of 1.9×10^{-17} M. Without labeling and the use of amplifiers, the detection method described here not only expands the application of MoS_2, but also offers a viable alternative for DNA analysis, which has the priority in sensitivity, simplicity, and costs. Moreover, the proposed sensing platform has good electrocatalytic activity, and can be extended to detect more targets, such as guanine and adenine, which further expands the application of MoS_2.

1. Introduction

MoS_2 is a type of transition metal sulfides, constructed by stacking covalently bound S–Mo–S through weak van der Waals interactions. As a 2D layer structure analogous of graphene, MoS_2 is becoming popular material nowadays attributed to its outstanding properties such as unusual optical properties (Goswami et al., 2013), robust mechanical properties and superior electrical performance (Ataca et al., 2011), and shows great promise in photovoltaics, nanoelectronics, energy storage, sensing, catalysis and even biology (Butler et al., 2013).

Just like graphene and bulk graphite, the anisotropic layered structure of MoS_2 leads to vastly different properties between the mono- or few-layer flakes and the bulk material. For example, the optical and electronic properties of the MoS_2 change with the decrease of the number of layers, mainly due to the electronic band transformation from indirect gap to direct gap (King et al., 2013). As a direct band gap semiconductor, MoS_2 with ultrathin layers displays strong photoluminescence and fluorescence quenching properties (Splendiani et al., 2010; Zhu et al., 2013). In addition to this, researches had elucidated that aromatic (e.g., pyridine, purine, etc.) and conjugated compounds could physisorpt on the basal plane of MoS_2 (Heckl et al., 1991; Moses et al., 2009).

In view of the above properties of MoS_2, a nucleic acid sequence detecting method with the single-layer MoS_2 nanosheet as sensing platform was proposed (Zhu et al., 2013). In that strategy, dye-labeled single-stranded DNA (ssDNA) probe (pDNA) could adsorb on the MoS_2 via the van der Waals force between nucleobases and the basal plane of MoS_2 nanosheet and then the fluorescence of the dye is quenched, while when a pDNA is hybridized with its complementary target DNA (cDNA), the dye-labeled probe could fall off the surface of MoS_2 because of its different affinity toward ssDNA versus double-stranded DNA (dsDNA), and resulting in regeneration of the fluorescence of the probe. The high affinity between ssDNA and MoS_2 nanosheet and the renewable property of the biosensing platform demonstrated that MoS_2 nanosheet is biocompatible and suitable for DNA analysis, and the fluorescence signal changes of the probe could be adopted for quantitative DNA assay.

However, though it is sensitive to the detection of the target molecule, this strategy needs oligonucleotide probes to be dye labeled, which markedly increases the time, complexity, and cost of the measurement. To overcome this shortcoming, more efforts should be made to develop label-free technologies based on the

* Corresponding authors. Tel.: +86 532 84022858; fax: +86 532 84023927.
E-mail address: taoyang@qust.edu.cn (T. Yang).

http://dx.doi.org/10.1016/j.bios.2014.09.030
0956-5663/

MoS_2 sensing platform. Among the various label-free analysis technologies, electrochemical assay is of special interest because of its low cost, high sensitivity, as well as inherent equipment simplicity (Wang et al., 2013).

Up to date, the electrochemical application of MoS_2 suffers from the limitation of its poor intrinsic conductivity (Meng et al., 2013). To improve the electronic conductivity and electrochemical activity of MoS_2, enormous attempts have been made, such as developing metallic 1T-MoS_2 by chemical exfoliation (Lukowski et al., 2013), reduction of the single-layer MoS_2 nanosheets (Wu et al., 2012), oxygen incorporation (Xie et al., 2013) and exploring carbon-based composites (Huang et al., 2014). However, the development of these materials has been encumbered by their complicated synthesis. Furthermore, the obtained MoS_2 with good conductivity are mostly used for improving the catalytic activity toward the oxygen-reduction reaction (ORR) and hydrogen-evolution reaction (HER) or used for lithium ion batteries (Chang and Chen, 2011; Zhu et al., 2014), the application of MoS_2 for electrochemical sensing has seldom been reported. In very recently, Huang et al. integrated MoS_2 with multi-walled carbon nanotube to overcome the low electronic conductivity and electrochemical activity of MoS_2, which was further combined with gold nanoparticles (to realize DNA immobilization via Au–S bonds self-assembly), and via enzyme multiple signal amplification to achieve sub-femtomolar DNA detection (Huang et al., 2014).

In this contribution, a label-free, electrochemical assay for detection of DNA immobilization and hybridization has been established directly on the MoS_2 sensing platform for the first time. The MoS_2 nanosheets were fabricated by a simple ultrasound exfoliation method, which is scalable and no distortion compared with mechanical cleavage and lithium intercalation, respectively (Coleman et al., 2011). In addition, and most importantly, this procedure allows the formation of thin-layer nanosheets of MoS_2 (nanoMoS_2) with enhanced electrochemical activity. As a classic electroactive indicator, methyl blue (MB) has been used for monitoring the changes of electrode surface induced by DNA immobilization and hybridization, which eliminates the tedious and costly fluorophore labeling step. Without labeling and the use of amplifiers, the detection method described here not only expands the application of MoS_2, but also offers a viable alternative for DNA analysis, which has the priority in sensitivity, simplicity, and costs.

The procedure for the detection is illustrated in Scheme 1. Immobilization of the pDNA can be achieved on the nanoMoS_2 modified electrode surface without any surface pre-treatment or functional bonding. The affinity for probe immobilization is ascribed to van der Waals force between nucleobases of ssDNA and the basal plane of nanoMoS_2, as reported previously (Zhu et al., 2013). The probe immobilization improves the electrochemical signal of MB. After probe being hybridized with the cDNA, and followed by a negative potential removal procedure (-0.7 V, 300 s), the obtained dsDNA leave the nanoMoS_2 surface, due to the different affinity of MoS_2 toward ssDNA and dsDNA, which brings decrease of the electrochemical signal of MB. So, based on the high electrochemical activity and specific affinity of nanoMoS_2, a label-free ultrasensitive DNA bioassay via signal changes of MB has been successfully developed.

2. Experimental

2.1. Apparatus and reagents

Electrochemical measurements were performed with a CHI 660D electrochemical workstation (Shanghai CH Instrument

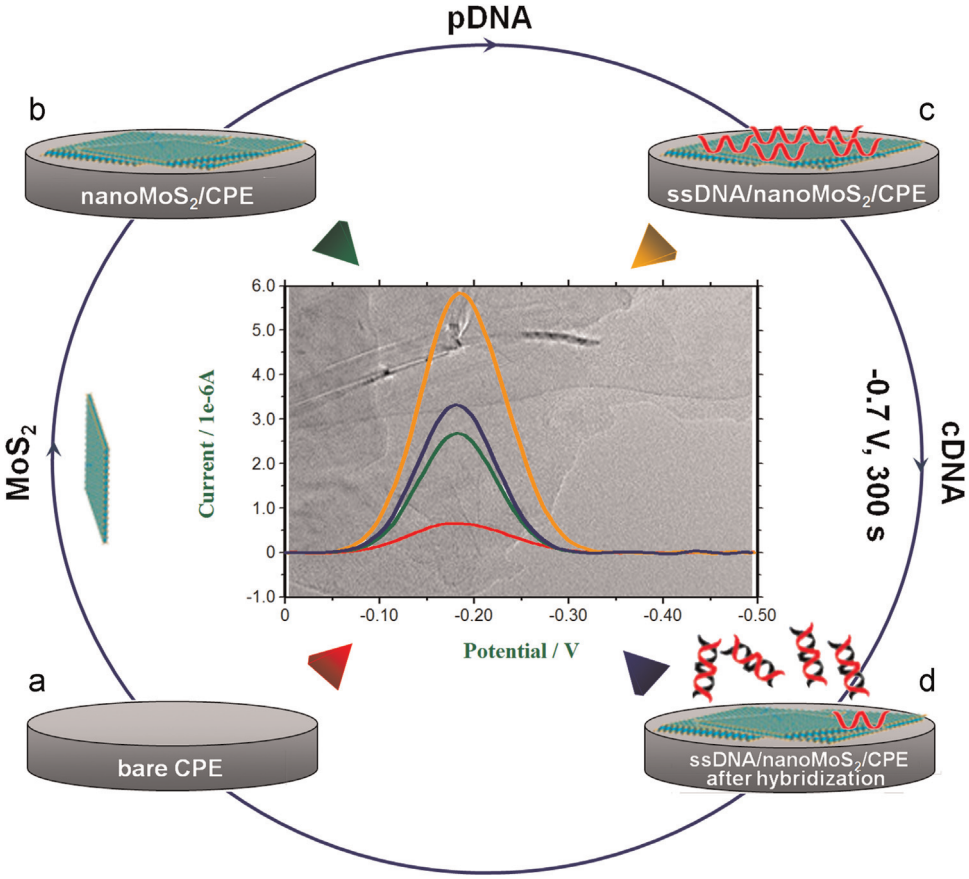

Scheme 1. Schematic illustration of the label-free electrochemical DNA assay: (a) bare carbon paste electrode (CPE), (b) nanoMoS_2 modified electrode (nanoMoS_2/CPE), (c) nanoMoS_2/CPE after pDNA immobilization (ssDNA/nanoMoS_2/CPE), and (d) ssDNA/nanoMoS_2/CPE after hybridization with cDNA.

Company, China) with a conventional three-electrode cell. A carbon paste electrode (CPE) or modified electrode was used as the working electrode, a saturated calomel as reference electrode (SCE) and a platinum wire as auxiliary electrode. The resulting MoS_2 was characterized by scanning electron microscopy (SEM, JSM-6700F machine, JEOL, Tokyo, Japan) and transmission electron microscopy (TEM, JEM 2100 transmission electron microscope).

The bulk MoS_2 was purchased from Tianjin Ba Si Fu Reagent Company (Tianjin, China). Carbon powder and Paraffin were obtained from Shanghai Colloid Laboratory and Shanghai Hua Ling Healing Appliance Factory, respectively. Tris(hydroxymethyl) aminomethane (Tris) and $Ru(NH_3)_6Cl_3$ were acquired from Sigma (St. Louis, MO, USA). Sodium dodecyl sulfate (SDS) was purchased from Shanghai Reagent Company (Shanghai, China) and used as received. N,N-Dimethylformamide (DMF) was provided by Tianjin Guang Cheng Reagent Company (Tianjin, China).

All the chemicals used were of analytical grade or higher and aqueous solutions were prepared with ultrapure water from an Aquapro ultrapure water system (Ever Young Enterprises Development. Co. Ltd., Chongqing, China).

The 23-base synthetic oligonucleotide probe (probe DNA, pDNA), its complementary DNA (cDNA, target DNA, namely a 23-base fragment of *tlh* gene sequence related to *Vibrio parahaemolyticus*), base mismatched DNA and non-complementary DNA were synthesized by Shanghai Sangon Biotechnology Co. Ltd. (Shanghai, China). The stock solutions are the same as those in Ref. Zhang et al. (2012), and their base sequences are listed in Table S1.

2.2. Preparation of the modified electrodes

The CPE was fabricated using the method reported by Yang et al. (2013b). The preparation of the $nanoMoS_2$ was carried out via a simple ultrasound exfoliation route. Detailed procedure is as follows: A certain amount of bulk MoS_2 was transferred into DMF, followed by ultrasonication for 22 h, and then a homogenous suspension of $nanoMoS_2$ was formed with the concentration of 0.5 g L^{-1}. 20.0 μL of the suspension was dripped on the fresh CPE surface and dried naturally in the air. The obtained electrode was denoted as $nanoMoS_2$/CPE. For comparison, bulk MoS_2/CPE was also fabricated with similar procedures, just without ultrasonication treatment.

2.3. Immobilization and hybridization

The immobilization of pDNA was performed via dropping 20.0 μL Tris–HCl buffer solution (pH 7.0, containing 1.0×10^{-6} M pDNA) onto the $nanoMoS_2$/CPE, and natural dried in the air. Before electrochemical analysis, the pDNA modified electrode should be washed extensively with ultrapure water to remove the unimmobilized oligonucleotides. After dropping 20.0 μL hybridization solutions (2× SSC buffer solution, pH 7.0, containing a certain amount of cDNA) onto the pDNA modified electrode, the hybridization reaction happened. After naturally dried in the air, the electrode was kept at −0.7 V for 300 s to release the dsDNA from the electrode surface (Yang et al., 2013a; Zhang et al., 2009), and thoroughly washed with 0.2% SDS solution was needed before measurements.

2.4. Electrochemical measurements

The cyclic voltammograms (CVs) were recorded in 1.0 M KCl solution containing 1.0 mM $K_3[Fe(CN)_6]$ and 1.0 mM $K_4[Fe(CN)_6]$ (1.0 mM $[Fe(CN)_6]^{3-/4-}$) and 1.0 M KCl containing 0.5 mM $Ru(NH_3)_6Cl_3$ (0.5 mM $[Ru(NH_3)_6]^{3+}$), respectively. In 1.0 mM $[Fe(CN)_6]^{3-/4-}$, the potential scanning range was from 0.6 V to −0.3 V with a scan rate of 0.1 Vs^{-1}; While in 0.5 mM $Ru(NH_3)_6{}^{3+}$, the cyclic voltammetry (CV) experiment was performed between 0.3 V and −0.7 V at a scan rate of 0.1 Vs^{-1}.

The differential pulse voltammogram (DPV) measurements were performed in Britton–Robinson (B–R) buffer solution (pH 6.0) containing 2.0×10^{-5} M MB. The pulse amplitude, pulse width, and pulse period were set as 0.05 V, 0.06 s and 0.2 s, respectively. The working electrodes were dipped into the MB solution for a given time to obtain reliable response of MB.

The reported result for every electrode in this assay was the mean value of three parallel measurements. All experiments were carried out at room temperature.

3. Result and discussion

3.1. Morphology characterization of MoS_2

SEM images of MoS_2 before and after ultrasound exfoliation are shown in Fig. 1. Without the ultrasonic treatment, the starting MoS_2 (bulk MoS_2, Fig. 1A) shows massive morphology and the diameter of it is about several microns. After 22 h of ultrasonication, $nanoMoS_2$ (Fig. 1B) with the lateral sizes of hundreds of nanometers were produced. The result indicates that both the lateral sizes and the thicknesses of layered MoS_2 can be reduced by the simple ultrasound exfoliation. TEM was used to further characterize the $nanoMoS_2$. From the TEM image (Fig. 1C), we can see that the $nanoMoS_2$ are of ultrathin nanosheet morphology and overlap each other, which is consistent with the SEM result.

3.2. Electrochemical characterization of MoS_2 modified electrodes

The electrochemical activity of the MoS_2 was investigated by CV in 1.0 M KCl containing 1.0 mM $[Fe(CN)_6]^{3-/4-}$ and shown in Fig. 2A. The bare CPE shows weak redox peak currents and wide ΔE_p (the difference of peak potentials) owing to its weak conductivity. After being modified with the bulk MoS_2, the effect is not obvious. This is because bulk MoS_2 has low electronic conductivity due to the poor interlayer electron transport. While after functionalization with the $nanoMoS_2$, the prepared $nanoMoS_2$/CPE exhibits dramatically increased redox peak currents, and the ΔE_p shrinks very obviously, which demonstrates that the obtained $nanoMoS_2$ has enhanced electrochemical activity. This phenomenon may be attributable to the anisotropic layered structure of MoS_2, whose electronic structures and electrochemical activity can be greatly affected by the thickness or layered nanostructure (Lee et al., 2011). The result that the electrochemical activity of MoS_2 can be greatly influenced by ultrasonication time provides further evidence in supporting the above explanation (see Supplementary material, Fig. S1).

For further confirmation about the high electrochemical activity of $nanoMoS_2$, the CV responses to the positively charged $[Ru(NH_3)_6]^{3+}$, a common DNA-binding and redox-active probe, at the CPE and the MoS_2 modified CPE are presented (see Supplementary material, Fig. S2). Similar to the results that obtained from negatively charged probe $[Fe(CN)_6]^{3-/4-}$, a pair of much higher redox peak of the positively charged probe is observed on $nanoMoS_2$/CPE than that on the CPE and bulk MoS_2/CPE, which conforms to our anticipation and confirms the above conclusion.

3.3. Analytical characteristics of the biosensor

To examine the DNA assay capability of the $nanoMoS_2$ sensing platform, the ability of immobilizing probe on the electrode surface was firstly studied. As a classic electroactive indicator widely adopted in DNA sensor, MB has been used for monitoring

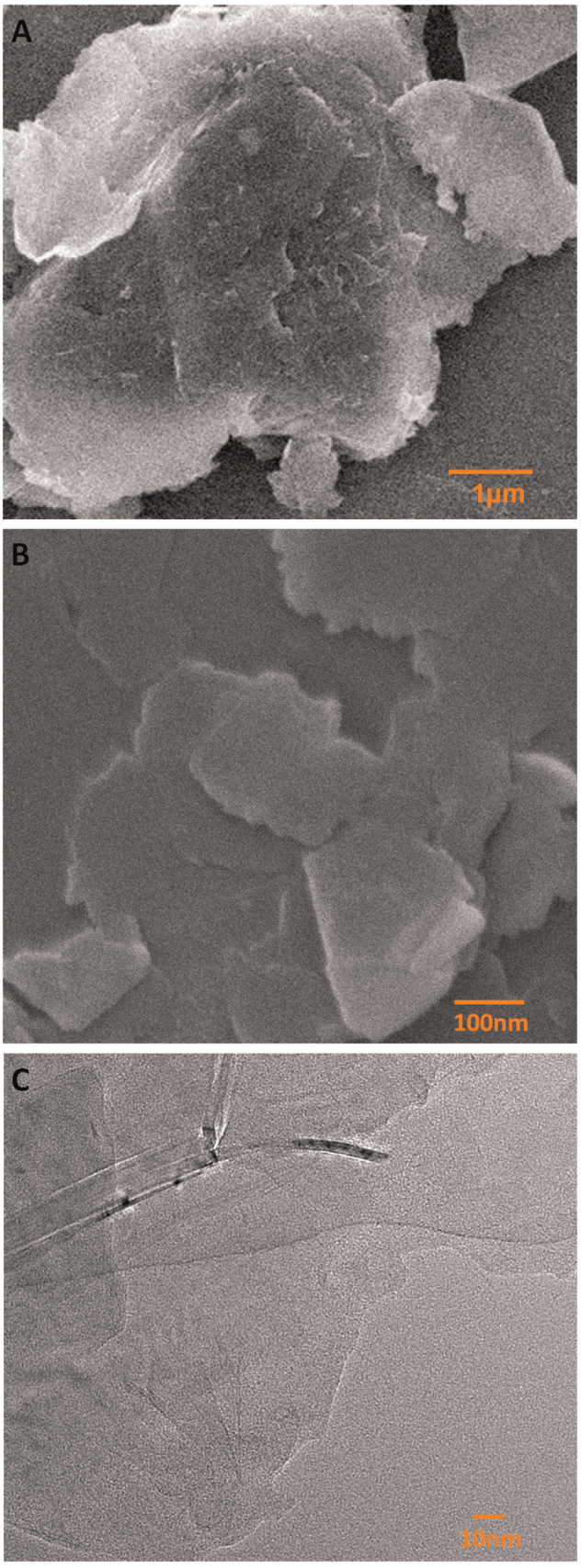

Fig. 1. The SEM images of the bulk MoS_2 (A) and nanoMoS_2 (B), and the TEM image of nanoMoS_2 (C).

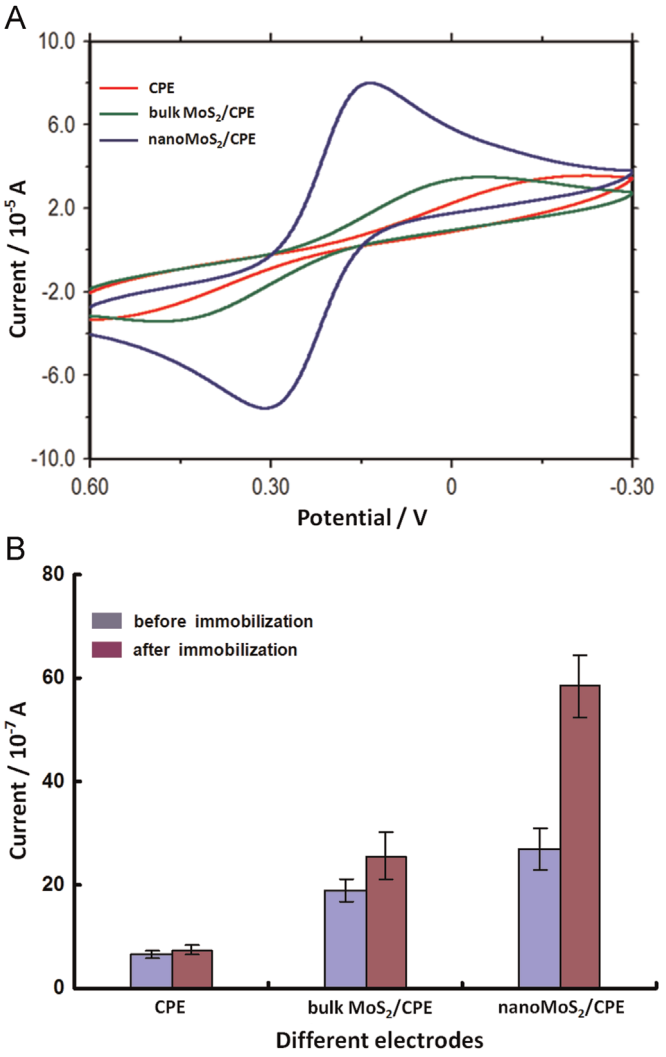

Fig. 2. (A) CV plots obtained at bare CPE, bulk MoS_2/CPE and nanoMoS_2/CPE in 1.0 M KCl containing 1.0 mM $[Fe(CN)_6]^{3-/4-}$; (B) DPV signals of 2.0×10^{-5} M MB at bare CPE, bulk MoS_2/CPE and nanoMoS_2/CPE before and after pDNA immobilization.

the changes of electrode surface induced by DNA immobilization and hybridization. The DPV signals of MB at the CPE and the MoS_2 modified CPE before and after pDNA immobilization are displayed in Fig. 2B (The corresponding DPV plots are shown in Supplementary material, Fig. S3.) From it, we can see that after the pDNA immobilization, an obvious increase of the reduction peak current value is observed on the nanoMoS_2/CPE. This is attributable to a large amount of MB accumulation occurring on the electrode surface, due to the strong affinity between MB and the free guanine bases exposed out of ssDNA, which indicates that pDNA has been successfully bounded to the nanoMoS_2 modified electrode surface. Compared with the nanoMoS_2/CPE, the change of the reduction peak current value of MB on the bulk MoS_2/CPE is much smaller, and for the bare CPE, the change is neglectable. This indicates the larger surface area and the higher electrochemical activity of nanoMoS_2 play an important role in effective immobilization of pDNA and enhancing the electric signal, which are the key factors to improve the detection sensitivity. Therefore, the nanoMoS_2 modified electrode could serve as favorable sensing platform for DNA immobilization. In addition to this, in comparison with CPE, the greatly enhanced reduction peak current of MB

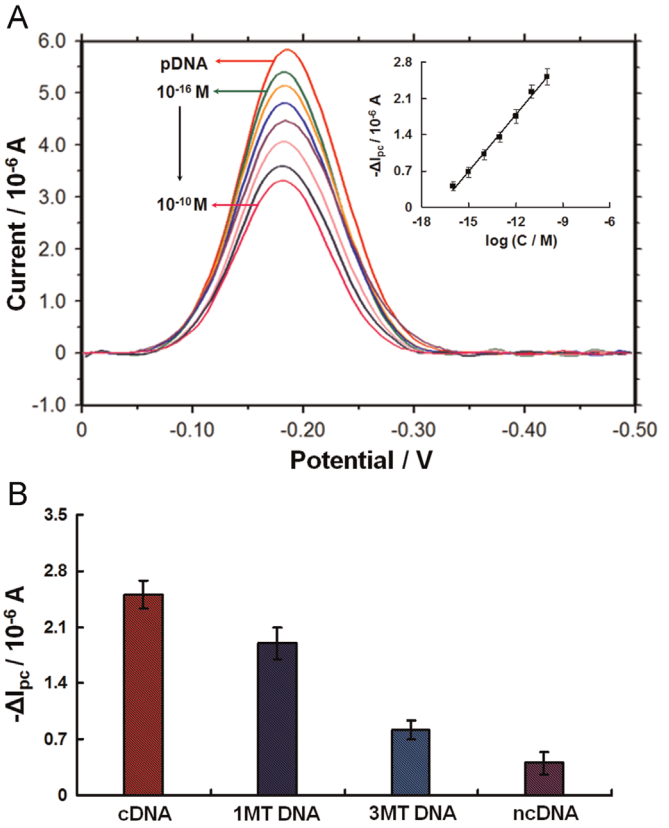

Fig. 3. (A) DPV plots of 2.0×10^{-5} M MB at pDNA (1.0×10^{-6} M) modified nanoMoS$_2$/CPE and that after hybridization with different concentrations of *tlh* gene sequence. Inset: The plot of $-\Delta I_{pc}$ versus the logarithm of *tlh* gene sequence concentrations; (B) comparison of hybridization signal changes for pDNA modified nanoMoS$_2$/CPE hybridized with cDNA, single-base mismatched DNA (1 MT DNA), three-base mismatched DNA (3 MT DNA), and non-complementary DNA (ncDNA). The detection concentrations of these sequences were all selected as 1.0×10^{-10} M.

on the nanoMoS$_2$/CPE also proves that the prepared nanoMoS$_2$ have high electrochemical activity.

Next, we investigated the specific hybridization capture of target DNA on the nanoMoS$_2$ sensing platform, and the synthetic sequence of the *tlh* gene segment related to *V. parahaemolyticus* was selected as the target DNA. As shown in Fig. 3A, after hybridization with the cDNA (10^{-10} M), the reduction peak current of MB decreases significantly. This is ascribed to the decrease of the amount of the remaining pDNA, which is caused by the releasing of the formed dsDNA helix from the surface of nanoMoS$_2$ modified electrode. The change of the signals shows an opposite tend with that in pDNA immobilization, and can be used as a strong proof for identifying that the pDNA have been successfully hybridized with its complementary sequence. Moreover, we can see that the reduction peak current decreases with increasing concentration of the target. The difference (namely ΔI_{pc}) between the reduction peak current value of MB at the ssDNA immobilized electrode and that after hybridization with cDNA is adopted as the measurement signal. There is a good linear relationship ($R^2=0.9948$) between ΔI_{pc} and the concentration of the target within a range of 1.0×10^{-16}–1.0×10^{-10} M, and the regression equation is $-\Delta I_{pc}/A = 0.3626 \log C/M + 6.133$. The detection limit is estimated to be 1.9×10^{-17} M with 3σ (where σ was the relative standard deviation of 11 parallel measurements of the blank solution), which is much lower than that of the other electrochemical sensing platform for the *tlh* gene sequence detection (Sun et al., 2012). Besides, the biosensor based on the nanoMoS$_2$ reveals good stability and reproducibility (details in Supplementary material). These results illustrate that the nanoMoS$_2$ modified electrode with high electrochemical activity is a promising electrochemical sensing platform for DNA immobilization and hybridization detection.

The specificity of the label-free bioassay of DNA hybridization was also investigated by measuring changes in the electrochemical current that occurred when hybridization with different DNA sequences (including single-base mismatched DNA (1 MT DNA), three-base mismatched DNA (3 MT DNA), and non-complementary DNA (ncDNA) sequences). As illustrated in Fig. 3B, the largest signal decrease is observed with the cDNA sequence, while a much lower signal change is seen with the 1 MT DNA sequence. The 3 MT DNA sequence produces an even lower signal change, and the signal change observed with the ncDNA sequence is the smallest and negligible. This demonstrates that the label-free electrochemical biosensor based on nanoMoS$_2$ sensing platform could distinguish mismatched and non-complementary DNA sequences.

3.4. Extended application

To further explore the biology applications of the prepared nanoMoS$_2$, we conducted the direct electrochemistry of adenine and guanine on the nanoMoS$_2$ modified electrode. The positively charged guanine and adenine could adsorb on the nanoMoS$_2$ surface not only via the van der Waals force, but also through electrostatic adsorption. For details, please see Supplementary material (Fig. S4). The result displays that the biosensor based on the nanoMoS$_2$ could detect guanine and adenine simultaneously. Compared with bulk MoS$_2$, the significantly improved electrocatalytic activity of nanoMoS$_2$ can be put down to its′ more active sites and higher electrochemical activity (Xie et al., 2013), which indicates the nanoMoS$_2$ show promising potentials in serving as excellent sensing platform for highly sensitive determination of guanine and adenine, or other biomolecules.

4. Conclusion

In summary, a new selective and sensitive electrochemical sensing platform for DNA assay based on the prepared nanoMoS$_2$ with high electrochemical activity has been developed. This assay system simultaneously gets rid of dye labeling and using amplifiers, which results in the decrease of the assay cost and the simplification of the operation. Moreover, the proposed sensing platform has good electrocatalytic activity, and can be extended to detect more targets, such as guanine and adenine, which further expands the application of MoS$_2$.

Acknowledgments

The authors are most grateful to the National Natural Science Foundation of China (no. 21275084, 41476083), Doctoral Foundation of the Ministry of Education of China (no. 20113719130001), Scientific and Technical Development Project of Qingdao (no. 12-1-4-3-(23)-jch), and Outstanding Adult-Young Scientific Research Encouraging Foundation of Shandong Province (no. BS2012CL013).

Appendix A. Supplementary materials

Supplementary data associated with this article can be found in the online version at http://dx.doi.org/10.1016/j.bios.2014.09.030.

References

Ataca, C., Şahin, H., Aktűrk, E., Ciraci, S., 2011. J. Phys. Chem. C 115, 3934–3941.

Butler, S.Z., Hollen, S.M., Cao, L.Y., Cui, Y., Gupta, J.A., Gutiérrez, H.R., Heinz, T.F., Hong, S.S., Huang, J.X., Ismach, A.F., Johnston-Halperin, E., Kuno, M., Plashnitsa, V.V., Robinson, R.D., Ruoff, R.S., Salahuddin, S., Shan, J., Shi, L., Spencer, M.G., Terrones, M., Windl, W., Goldberger, J.E., 2013. ACS Nano 7, 2898–2926.

Chang, K., Chen, W.X., 2011. ACS Nano 5, 4720–4728.

Coleman, J.N., Lotya, M., O'Neill, A., Bergin, S.D., King, P.J., Khan, U., Young, K., Gaucher, A., De, S., Smith, R.J., Shvets, I.V., Arora, S.K., Stanton, G., Kim, H.Y., Lee, K., Kim, G.T., Duesberg, G.S., Hallam, T., Boland, J.J., Wang, J.J., Donegan, J.F., Grunlan, J.C., Moriarty, G., Shmeliov, A., Nicholls, R.J., Perkins, J.M., Grieveson, E. M., Theuwissen, K., McComb, D.W., Nellist, P.D., Nicolosi, V., 2011. Science 331, 568–571.

Goswami, N., Giri, A., Pal, S.K., 2013. Langmuir 29, 11471–11478.

Heckl, W.M., Smith, D.P.E., Binnig, G., Klagges, H., Hansch, T.W., Maddocks, J., 1991. Proc. Natl. Acad. Sci. USA 88, 8003–8005.

Huang, K.J., Liu, Y.J., Wang, H.B., Wang, Y.Y., Liu, Y.M., 2014. Biosens. Bioelectron. 55, 195–202.

King, L.A., Zhao, W.J., Chhowalla, M., Rileya, D.J., Eda, G., 2013. J. Mater. Chem. A 1, 8935–8941.

Lee, K., Kim, H.Y., Lotya, M., Coleman, J.N., Kim, G.T., Duesberg, G.S., 2011. Adv. Mater. 23, 4178–4182.

Lukowski, M.A., Daniel, A.S., Meng, F., Forticaux, A., Li, L., Jin, S., 2013. J. Am. Chem. Soc. 135, 10274–10277.

Meng, F.K., Li, J.T., Cushing, S.K., Zhi, M.J., Wu, N.Q., 2013. J. Am. Chem. Soc. 135, 10286–10289.

Moses, P.G., Mortensen, J.J., Lundqvist, B.I., Norskov, J.K., 2009. J. Chem. Phys. 130, 104709.

Splendiani, A., Sun, L., Zhang, Y., Li, T., Kim, J., Chim, C.Y., Galli, G., Wang, F., 2010. Nano Lett. 10, 1271–1275.

Sun, W., Zhang, Y.Y., Ju, X.M., Li, G.J., Gao, H.W., Sun, Z.F., 2012. Anal. Chim. Acta 752, 39–44.

Wang, Q.P., Zheng, H.Y., Gao, X.Y., Lin, Z.Y., Chen, G.N., 2013. Chem. Commun. 49, 11418–11420.

Wu, S.X., Zeng, Z.Y., He, Q.Y., Wang, Z.J., Wang, S.J., Du, Y.P., Yin, Z.Y., Sun, X.P., Chen, W., Zhang, H., 2012. Small 8, 2264–2270.

Xie, J.F., Zhang, J.J., Li, S., Grote, F., Zhang, X.D., Zhang, H., Wang, R.X., Lei, Y., Pan, B.C., Xie, Y., 2013. J. Am. Chem. Soc. 135, 17881–17888.

Yang, T., Guan, Q., Guo, X.H., Meng, L., Du, M., Jiao, K., 2013a. Anal. Chem. 85, 1358–1366.

Yang, T., Guan, Q., Li, Q.H., Meng, L., Wang, L.L., Liu, C.X., Jiao, K., 2013b. J. Mater. Chem. B 1, 2926–2933.

Zhang, W., Yang, T., Jiao, K., 2012. Biosens. Bioelectron. 31, 182–189.

Zhang, X.Z., Jiao, K., Liu, S.F., Hu, Y.W., 2009. Anal. Chem. 81, 6006–6012.

Zhu, C.B., Mu, X.K., van Aken, P.A., Yu, Y., Maier, J., 2014. Angew. Chem. Int. Ed. 53, 2152–2156.

Zhu, C.F., Zeng, Z.Y., Li, H., Li, F., Fan, C.H., Zhang, H., 2013. J. Am. Chem. Soc. 135, 5998–6001.